J. Mol. Model. **2000**, *6*, 563 – 574

Journal of Molecular Modeling

FULL PAPER

Ab initio Models for Six-Center Multiple Proton Exchange and Ion Pair Formation Assisted by Lewis Acids

Nicolaas J.R. van Eikema Hommes[1], Dietmar Heidrich[2], and Paul von Ragué Schleyer[1]

[1]Computer-Chemie-Centrum, Institut für Organische Chemie, Universität Erlangen-Nürnberg, D-91052 Erlangen, Germany. E-mail: schleyer@chemie.uni-erlangen.de

[2]Institut für Physikalische und Theoretische Chemie der Fakultät für Chemie und Mineralogie, Universität Leipzig, D-04109 Leipzig, Germany. E-mail: heidrich@informatik.uni-leipzig.de

Received: 6 August 1999/ Accepted: 9 June 2000/ Published: 20 September 2000

Abstract High level ab initio and density functional calculations, extrapolated to QCISD(T)/6-311+G(3df,2p)//MP2/6-31+G**+ZPE, reveal that cyclic ion pairs can form in the hydrogen bonded complexes of haloboric acids BH_nX_{3-n}–HX, X=F, Cl, with Lewis bases HX, H_2O, CH_3OH, and NH_3, even in isolation (e.g., in the gas phase). The intrinsic acidities (deprotonation energies) required for protonation of these bases with formation of gas phase ion pairs are calculated to be <295 kcal/mol for water, <301 kcal/mol for methanol, and <306 kcal/mol for ammonia; such values are common for acidic sites in zeolites. All gas phase ion pairs prefer symmetric bidentate or tridentate structures. In the other cases where hydrogen bonded complexes prevail, symmetric ion pair-like transition structures for multiple hydrogen exchange are computed.

Keywords Gas phase ion pairs, Multiple proton exchange, Ab initio calculations, Density functional calculations

Introduction

Ionic intermediates resulting from hydrogen (“proton”) transfer dominate the solution chemistry of Brønsted acids and bases.[1] However, stable ion pairs are relatively rare in the gas phase: $(CH_3)_3NH^+ Br^-$ is one of the few examples.[2] The reason is obvious: charge separation is strongly endothermic, and this energetic disadvantage is not compensated as it is in solution. In contrast, computational studies have shown that proton transfer reactions in hydrogen bonded molecular complexes (MC) often involve zwitterionic, i.e., ion pair like, transition structures (TS).[3] A good example is the degenerate hydrogen exchange between carboxylic acids and amines, as shown in Figure 1 for formic acid and ammonia.

The cyclic zwitterion serves as the transition structure for double hydrogen transfer, which proceeds in one-step in the gas phase.[3] Despite the large degree of charge separation, the activation barrier is rather small. A similar result was obtained for electrophilic aromatic substitution involving benzene and HF-BF_3, [4] although a higher barrier was calculated.[4c] Even this acid was not strong enough to protonate a benzene carbon and to form a stable ion pair in the gas phase. Instead, the “sigma-complex” depicted in

Correspondence to: D. Heidrich and P. von Ragué Schleyer

Figure 1 *Hydrogen exchange between formic acid and ammonia*

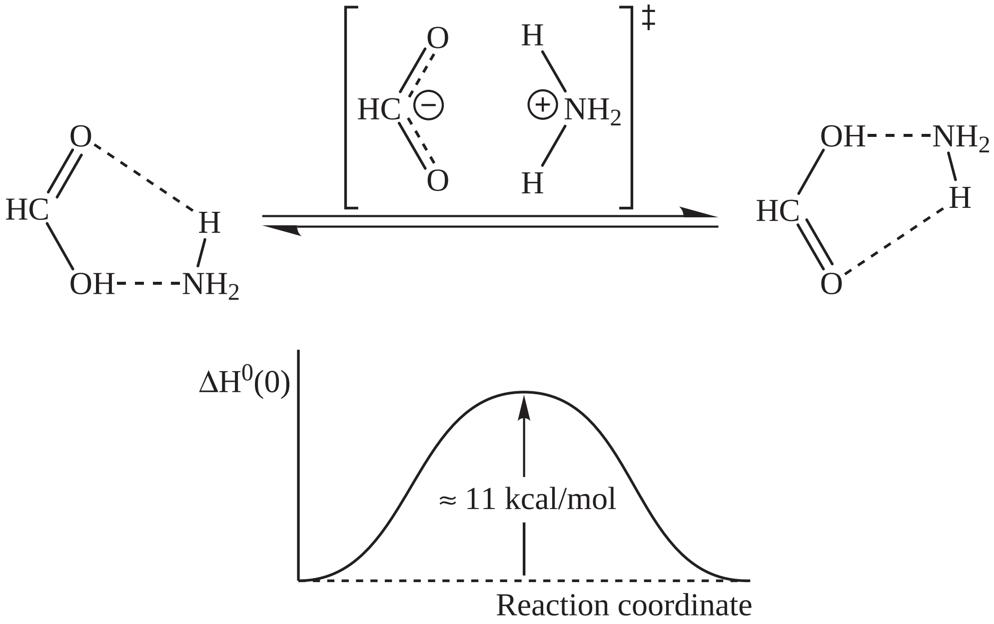

Figure 2a, (which is an ion pair in solution and in the solid state)[1b] corresponded to the transition structure for double hydrogen exchange in the gas phase. Further examples involve the cyclic molecular complex and the transition structure for double hydrogen transfer computed for $AlF_3(HF)_2$ [5] as well as similar systems containing water, $AlF_3(H_2O)_2$, $AlCl_3(H_2O)_2$, and $AlF_3(H_2O)_3$. These also were computed to prefer cyclic hydrogen bonded complexes over ion pairs.[6]

Conditions rather similar to the gas phase are present in zeolite cages containing only a single substrate molecule. The formation of ion pairs, observed experimentally for ammonia (Figure 2b) and amines at a strongly acidic site,[7] has been corroborated by high level computations.[8, 9]

Results of experiments involving water and, in particular, methanol in zeolites were ambiguous; different interpretations have been offered.[10] However, several recent high level calculations agree that ion pairs should not be formed.[11] The methoxonium ion comprises part of a low energy proton exchange transition structure, which connects two hydrogen-bonded molecular adsorption complexes along a broad and shallow potential well. The small potential energy barrier, below 3 kcal/mol, "almost disappears" [11c] when the zero point energy correction is included. A similar situation is encountered for water adsorbed on Brønsted sites in zeolites.[12, 13]

Our previous work on multiple hydrogen exchange [3] suggested that cyclic ion pairs, i.e. minima instead of transition structures, might be formed in isolation when strong, bifunctional acids interact with strongly basic molecules that contain exchangeable hydrogen atoms. Indeed, Gadre et al. recently found a stable ion pair structure for NH_4^+ BF_4^-.[14] The present investigation, involving stronger boron containing acids, defines the borderline between hydrogen bonded systems, i.e., those exhibiting hydrogen exchange via zwitterionic transition structures, and systems that form contact ion pairs. Factors that determine the preference for ion pair formation are identified.

Methods

Calculations were performed using the Gaussian-98 program suite.[15] All structures were fully optimized at the MP2(full)/6-31+G** and B3LYP/6-311+G** levels, with no constraints other than symmetry, and were characterized as minima, tran-

Figure 2 *Transition structure vs. ion pairs. (***a***) Transition structure for proton exchange exchange in benzene-*HBF_4*; (***b***) Ion pair of ammonia and a zeolite acidic site*

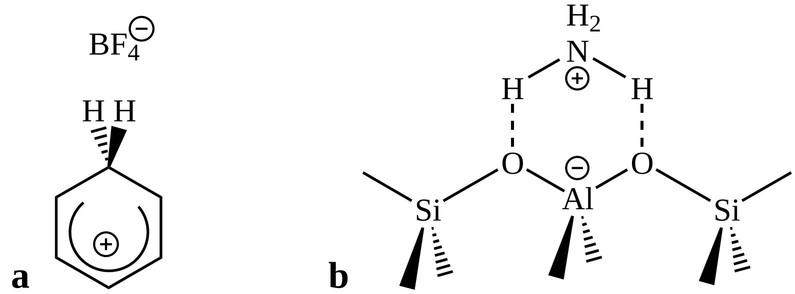

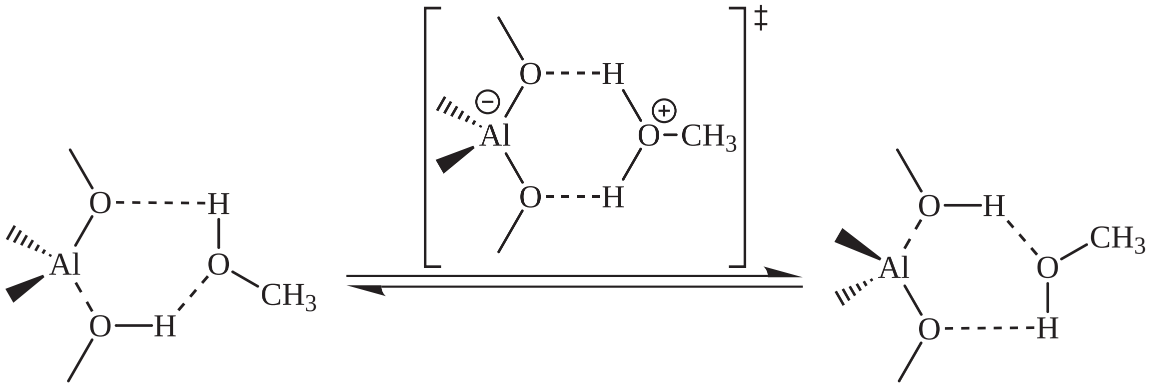

Figure 3 *Hydrogen exchange between methanol and a zeolite acidic site*

sition structures or higher order saddle points by calculating the vibrational frequencies. Zero point vibrational energies were scaled by factors of 0.945 (MP2) and 0.98 (B3LYP). Energies were computed using the MP2/6-31+G** geometries at QCISD(T)/6-311+G** and at MP2/6-311+G(3df,2p). An extrapolation procedure similar to the G2-MP2 scheme of Curtiss et al.[16] gave energy estimates at the effective QCISD(T)/6-311+G(3df,2p)//MP2(full)/6-31+G** level, as follows:

$$E_{\text{"QCISD(T)/6-311+G(3df,2p)"}} = E_{\text{QCISD(T)/6-311+G**}} + (E_{\text{MP2/6-311+G(3df,2p)}} - E_{\text{MP2/6-311+G**}}) \quad (1)$$

We refer to this level as “QCISD(T)”. Unless indicated otherwise, relative energies have been evaluated by this procedure and include scaled MP2(full)/6-31+G** zero point vibrational energy corrections (ΔZPE), i.e., $\Delta H^0(0) = \Delta E_{\text{"QCISD(T)/6-311+G(3df,2p)"//MP2(fu)/6-31+G**}} + \Delta ZPE$. The “higher level corrections” of G2 theory were not applied, since no open shell systems are involved in the present work.

Charges and bond orders were calculated using the natural population analysis (NPA), natural bond orbital analysis (NBO), and natural localized molecular orbital (NLMO) methods,[17] based on the QCISD density. Relative energies (kcal/mol), corrected for tero point vibrational energy differences are given in Table 1.

Results and discussion

Haloboric acids

The acidity of hydrogen halides is enhanced significantly by complexation to boron hydrides or to boron halides. For example, the computed deprotonation energy $\Delta H^o_{DP}(0)$ of HF **1**, 372 kcal/mol, is reduced to 293 kcal/mol upon complexation to BF_3 **12**. The deprotonation energies of the fluoroboric and chloroboric acids considered in this study range from 290 kcal/mol to 308 kcal/mol. Interestingly, this range coincides with the acidities of zeolite and zeolite cluster models (c.f. ref. [9]). Deprotonation energies of zeolites, determined spectroscopically, range from 272 to 318 kcal/mol.[18]

The acidities of the complexes increase with the number of halogens bound to boron. However, fluorine and chlorine show different behavior. For X = F, the deprotonation energies of H_3BFH **16** (308 kcal/mol) to H_2BF_2H **18** (307 kcal/mol) are nearly the same, but the introduction of the third and, in particular, the fourth fluorine atom result in large changes (HBF_3H **21**: 301 kcal/mol; BF_4H **25**: 293 kcal/mol). For chlorine, the deprotonation energy decreases from 301 kcal/mol for H_3BClH **28** to 296 kcal/mol (H_2BCl_2H **30**) to 292 kcal/mol ($HBCl_3H$ **33**) to 290 kcal/mol for BCl_4H **37**. The larger chlorine atoms distribute the negative charge more effectively than the smaller fluorines. A technical consequence is that **30** is an appropriate model for **37**, whereas **18** is not a suitable model for **25**.

While the haloboric anions are strongly bound structures, the corresponding acids only are weak complexes of hydrogen halide and boron halide. Our calculated complexation energies range from 1.1 kcal/mol for HBF_2–FH **18** to 3.0 kcal/mol for BF_3–FH **25**. The latter value agrees well with the literature range of 3 to 4 kcal/mol.[19] Hence, the acidity of the haloboric acids is controlled by the stability of the corresponding anions. The negative charge, which is located on the halogen atoms, results in significantly longer boron halogen bonds in the haloboric anions than in the neutral haloboranes. The extent of bond elongation decreases with increasing number of halogens.

Hydrogen shifts within the haloboric acids involve compact, symmetric transition structures of the Y_2BX_2H type (**20**, **23**, **27**, **32**, **35**, **39**, X = F, Cl; Y = H, X). The migrating proton occupies a “bridging” position between two halogen atoms, X. The anionic Y_2BX_2 moieties in these transition structures resemble the corresponding free haloboric anions $Y_2BX_2^-$. However, the B-X bonds (i.e., the bonds to the halogens bridged by the migrating hydrogen) are even longer than in the “free” haloboric anions. The more acute X-B-X angles suggest “ring strain” in the cyclic transition structures. Indeed, the activation barriers are relatively large and increase with increasing number of boron-bound halogens, e.g., 16 kcal/mol for H_2BCl_2H **32**, 21.7 kcal/mol for $ClHBCl_2H$ **35**, and 26 kcal/mol for Cl_2BCl_2H **39**. Interestingly, this trend is opposite to that of the deprotonation energies, which *decrease* with increasing number of halogens. Increasing ring strain (viz. deviations of the Cl-B-Cl angle from the optimum valence angle) in the transition structures is likely to be responsible for this.

"Tridentate" structures with the migrating proton bridging three halogens, e.g., **24** or **36**, are conceivable, but these are second order saddle points, significantly higher in energy than the corresponding "bidentate" transition structures. Hence, they are not pertinent chemically, in contrast to the tridentate structures involving water or ammonia.

The BH_2X and BHX_2 systems not only serve as models for the BX_3 complexes, but also are relevant for the chemistry of the mono- and dihaloboranes. Recently, the microwave structures of the BH_2Cl and BH_2F monohaloboranes [20] were compared with high level ab initio geometries.[21]

Stabilities: ion pairs vs. transition structures

The haloboric acids with two or more halogens may form cyclic complexes with hydrogen containing bases. We consider a set of molecules of increasing basicity, HF, HCl, H_2O, CH_3OH, and NH_3. Both asymmetric structures, consisting of hydrogen bonded subunits, and more symmetric structures, with pairs of equivalent H–X and H–O or H–N bonds, are conceivable for the acid-base complexes, $Y_2BX\text{-}(XH)_2$, $Y_2BX\text{-}XH\text{-}H_2O$, $Y_2BX\text{-}XH\text{-}HOCH_3$, and $Y_2BX\text{-}XH\text{-}NH_3$, X = F, Cl; Y = H, X. The more symmetric species may represent transition structures for double hydrogen exchange or may be stable ion pairs resulting from protonation of the base. In addition, bidentate and tridentate bonding is possible in the complexes of NH_3 or H_2O with haloboric acids that contain three or four halogens, see figure 4.

The most important factors that determine the nature of such species are the relative strengths of the acids and of the bases. We define the proton transfer enthalpy $\Delta H^0_{PT}(0)$, required for the formation of an infinitely separated ion pair, as the difference between the deprotonation enthalpy $\Delta H^0_{DP}(0)$ of the acid (which equals the proton affinity of the corresponding anion) and the proton affinity $\Delta H^0_{PA}(0)$ of the base:

$$\Delta H^0_{PT}(0) = H^0_{DP}(0)[\text{acid}] - H^0_{PA}(0)[\text{base}] \qquad (2)$$

Other interactions, e.g., the Coulomb attraction between the ions and the strength and number of the hydrogen bonds, contribute to the stability of the complexes, but the proton transfer enthalpies nevertheless are useful guidelines. Figure 5 summarizes the relationship between the acid deprotonation enthalpies $\Delta H^0_{DP}(0)$ and the proton transfer enthalpies $\Delta H^0_{PT}(0)$. For comparison, literature values,[3] as well as some complexes of ammonia with carboxylic acids of increasing strength,[22] are included. Solid dots represent cases where stable ion pairs prevail, while open circles indicate that the hydrogen bonded molecular complexes are more stable than the related symmetric forms, which are transition structures for hydrogen transfer.

Figure 5 shows points along parallel lines for the bases, H_2O (top), CH_3OH (middle), and NH_3 (bottom), combined with the acids. The highest solid dot in each set (**74**, **65**, and **54**) indicates the minimum acidity (largest deprotonation energy) of the acids which leads to the formation of anion pair. The only "disorder" is found in the water set (**67** vs. **74**), reflecting the change from ClH to FH acidity. Figure 5 reveals the intrinsic acidity required to form an ion pair in the gas phase by protonating a given base. Thus, the onsets of ion pair formation $\Delta H_{DP}(0)$ are (in kcal/mol) < 295 for H_2O, < 301 for CH_3OH, and < 307 for NH_3.

All haloboric acids, even those of low intrinsic acidity, i.e., with only two halogens, form stable ion pairs with NH_3, the strongest base considered in this study. (Our computed proton affinity is 202.7 kcal/mol, the experimental value is 202.1 kcal/mol) [23] No additional minima corresponding to hydrogen bonded molecular complexes, similar to those with HX, $(HX)_2$, and formic acid,[3] could be located. The ion pairs are 19 to 27 kcal/mol more stable than the separated monomers (see Table 1); the chlorine-containing species have somewhat higher binding energies.

The proton transfer energies range from 89 kcal/mol for $BF_4^- NH_4^+$ **70** to 104 kcal/mol for $H_2BF_2^- NH_4^+$ **54**. $BCl_4^- NH_4^+$, which we did not consider explicitly in this study, has a proton transfer energy of 86 kcal/mol. However, no ion pair is formed for $NH_3(HCl)_2$,[3] even though the proton transfer energy is only 4 kcal/mol higher than for **54**. The fluorocarboxylic acids also do not form gas phase ion pairs with ammonia, but give hydrogen bonded complexes instead.

The character of the complexes of the haloboric acids with water depends on the halogens. Stable ion pairs **74**, (**75**), **79**, and **83** are formed with the chlorine containing acids H_2BCl_2H **30**, $HBCl_3H$ **33**, and BCl_4H **37**. The binding energies are lower than in the corresponding ion pairs with NH_3 (6 kcal/mol for **75** and **79**, 2 kcal/mol for **83**). Surprisingly, the stability order of the ion pairs is opposite to the order of the proton transfer energies. On the other hand, the fluoroboric acids form hydrogen bonded complexes **52**, **59**, and **67** with water. The corresponding symmetric transition structures **53**, **61**,

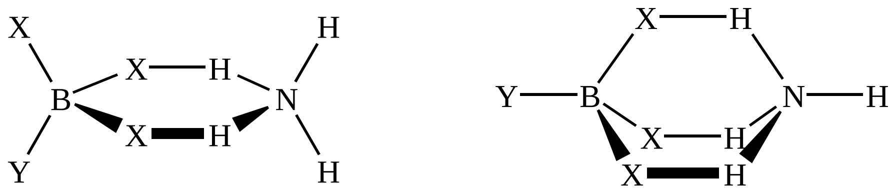

Figure 4 *Bidentate and tridentate bonding between haloboric acids (Y=H,X) and ammonia*

Figure 5 *Proton transfer enthalpy vs acid deprotonation enthalpy for acids of increasing strength and the bases NH_3, CH_3OH, and H_2O*

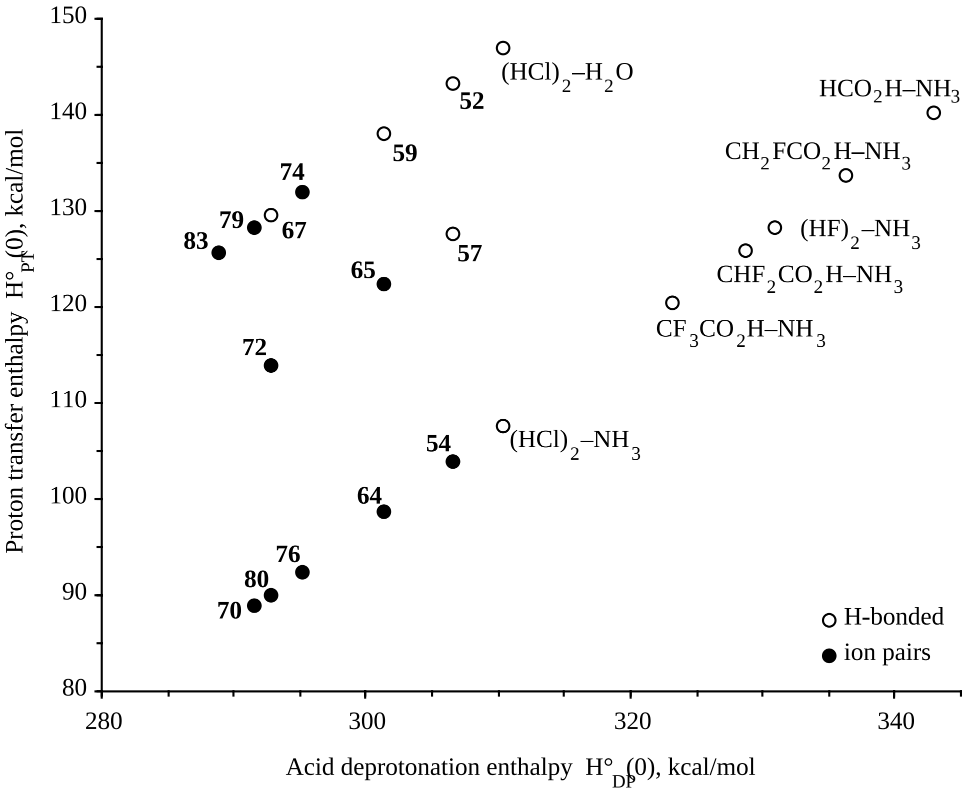

and **68** for multiple hydrogen exchange have activation barriers of only 5 to 7 kcal/mol, i.e., well below the binding energies, 11 to 13 kcal/mol, of the complexes. Note the "disorder" of point **67** and **74** in Fig. 5: BF_4H **25**, which forms hydrogen bonded complex **67**, has a higher intrinsic acidity than H_2BCl_2H **30**, for which we compute stable ion pair **74** with water. The stronger F-H bond, compared to the Cl-H bond, prevents proton transfer.

In view of the importance of methanol (**7**) in zeolite chemistry,[11] we also considered its complexes with fluoroboric acids. The calculated proton affinity for **7**, 179 kcal/mol,[23] lies between the values for water (**3**) (163.3 kcal/mol) and ammonia (**5**) (202.7 kcal/mol), so that the behavior of CH_3OH might be intermediate. Indeed, methanol forms a hydrogen bonded complex **57** with H_2BF_2H **18**, while the stronger acids HBF_3H **21** and BF_4H **25** give stable ion pairs **65** and **72**. The corresponding symmetrical structures **66** and **73** are marginally less stable. Hence, the superposition of **72** and **73** represents the actual nonrigid minimum structure of the ion pair $CH_3OH_2^+$ BF_4^-. An interesting aspect of the geometries of **65** (**66**) and **72** (**73**) is the proximity (2.43 and 2.45 Å, respectively) of one of the methyl hydrogens of the methoxonium cation to the third fluorine atom at boron. This additional interaction favors the ion pair over an alternative hydrogen bonded structure. The stability of the ion pair vs. the monomers is 15.4 kcal/mol.

Ion pairs with three instead of two X-H interactions are possible for the complexes with HBX_3H and BX_4H type acids. These tridentate structures (**62**, **64**, **69**, **71**, **79**, **81**, and **83**) are second order saddle points at MP2(full)/6-31+G**. However, the only slightly more stable corresponding bidentate minima (**63**, **70**, **78**, **80** and **82**) or transition structures (**61** and **68**) have essentially the same stability at the higher "G2" level.

Not unexpectedly, the rather weak bases HF and HCl (computed proton affinities are 121 and 139 kcal/mol, respectively) [3] only form weakly hydrogen bonded complexes of the YHBX-XH-XH (X=F,Cl; Y=H,X) type.[24] For X=F, these complexes **40** and **43** are 4.1 and 7.6 kcal/mol more stable than separated HF and $YHBF_2H$ species; for X=Cl, both complexes are 3.4 kcal/mol more stable. The binding energies in such complexes are not additive, but are larger than the sum of the binding energies for YHBX-XH and $(HX)_2$. Symmetric bidentate structures again correspond to transition structures for multiple hydrogen transfer, but the activation barriers, ranging from 10 to 19 kcal/mol, are significantly higher than for the H_2O containing systems.

Structures

The computed structures for the six-membered B-X-H-Z-H-X rings (X = F, Cl; Z = X, O, N) in the bidentate ion pairs and in the hydrogen exchange transition structures are strongly folded at the X–X axis (e.g., 50° in H_2BF_2-NH_4 **54** and even 73° in H_2BCl_2-NH_4 **76**). These structures have staggered configurations around the B–X bonds, which minimize the repulsion between the substituents on boron and the halogen

Table 1 *Relative energies (kcal/mol), corrected for zero point vibrational energy differences*

Species		**MP2(fu)/ 6-31+G****	**MP2/ 6-311+G****	**QCISD(T)/ 6-311+G****	**MP2/ 6-311+G(3df.2p)**	**"QCISD(T)"/ 6-311+G(3df.2p)**	**B3LYP/ 6-311+G****
H_3O^+	**4**	164.75	164.66	165.98	161.98	163.31	163.37
NH_4^+	**6**	205.65	204.29	205.63	201.37	202.71	202.91
$CH_3OH_2^+$	**8**	180.20	180.21	181.73	177.48	178.99	179.26
H_3B+HF		1.24	1.12	1.29	1.32	1.49	0.86
H_3B-FH stagg.	**16a**	0.00	0.00	0.00	0.00	0.00	0.00
H_3B-FH ecl.	**21**	-0.09	-0.12	-0.12	-0.15	-0.15	0.00
H_3BF^-	**22**	307.86	309.34	311.05	305.96	307.66	306.56
H_2BF+HF		1.92	1.55	1.66	1.64	1.75	1.18
H_2BF-FH	**18**	0.00	0.00	0.00	0.00	0.00	0.00
$H_2BF_2^-$	**19**	304.48	307.51	309.37	304.68	306.54	304.95
H_2BF_2H	**20**	17.63	19.63	20.40	18.36	19.13	19.24
HBF_2+HF		1.38	1.00	1.18	0.94	1.12	1.44
HBF_2-FH	**21**	0.00	0.00	0.00	0.00	0.00	0.00
HBF_3^-	**22**	297.57	301.85	303.64	299.51	301.31	300.28
$HFBF_2H$	**23**	21.04	23.27	23.96	21.91	22.60	23.55
HBF_3H	**24**	61.70	66.80	67.54	62.34	63.08	62.96
BF_3+HF		3.37	2.78	3.05	2.73	3.00	2.03
BF_3-FH	**25**	0.00	0.00	0.00	0.00	0.00	0.00
BF_4^-	**26**	287.97	292.86	294.51	291.15	292.80	290.32
F_2BF_2H	**27**	22.86	25.08	25.71	23.66	24.29	24.38
H_3B+HCl		0.99	1.56	1.57	1.79	1.81	0.30
H_3B-HCl	**28**	0.00	0.00	0.00	0.00	0.00	0.00
H_3BCl-	**29**	301.70	300.77	303.64	297.76	300.63	299.75
H_2BCl+HCl		1.13	1.26	1.15	1.48	1.38	0.37
H_2BCl-ClH	**30**	0.00	0.00	0.00	0.00	0.00	0.00
$H_2BCl_2^-$	**31**	295.62	295.13	298.73	291.58	295.19	294.96
H_2BCl_2H	**32**	20.67	15.01	16.92	14.12	16.02	16.97
$HBCl_2$+HCl		1.40	1.55	1.47	1.79	1.70	0.07
$HBCl_2$-ClH	**33**	0.00	0.00	0.00	0.00	0.00	0.00
$HBCl_3^-$	**34**	291.54	291.38	295.37	287.61	291.60	291.47
$HClBCl_2H$	**35**	26.14	20.54	22.73	19.49	21.67	22.59
$HBCl_3H$	**36**	61.61	55.08	57.60	50.44	52.95	54.83
BCl_3+HCl		1.81	1.98	1.90	2.26	2.17	0.06
BCl_3-ClH	**37**	0.00	0.00	0.00	0.00	0.00	0.00
BCl_4-	**38**	288.36	288.47	292.64	284.72	288.89	289.12
Cl_2BCl_2H	**39**	30.07	24.62	26.97	23.65	26.01	27.11
H_2BF+2HF		6.00	4.65	4.79	5.67	5.82	5.16
H_2BF-FH-FH	**40**	0.00	0.00	0.00	0.00	0.00	0.00
H_2BF_2 H_2F	**41**	7.97	9.91	10.80	8.83	9.72	8.86
H_2BF_2 H_2F	**42**	7.90	9.93	10.83	8.68	9.58	8.75
HBF_2+2HF		8.89	7.65	7.94	8.46	8.76	7.62
HBF_2-FH-FH	**43**	0.00	0.00	0.00	0.00	0.00	0.00
$HFBF_2H_2F$	**44**	11.16	13.52	14.29	12.36	13.13	12.08
H_2BCl+2HCl		4.00	3.96	3.56	5.11	4.71	1.80
H_2BCl-ClH-ClH	**45**	0.00	0.00	0.00	0.00	0.00	0.00
H_2BCl-ClH-ClH	**46**	0.28	0.42	0.40	0.59	0.56	0.21
$H_2BCl_2H_2Cl$	**47**	17.57	10.99	13.88	9.61	12.51	11.60
$H_2BCl_2H_2Cl$	**48**	19.55	13.24	15.91	11.03	13.69	12.91
$HBCl_2$+2HCl		4.38	4.38	4.08	5.43	5.13	1.54
$HBCl_2$-ClH-ClH	**49**	0.00	0.00	0.00	0.00	0.00	0.00
$HClBCl_2H_2Cl$	**50**	23.73	17.21	20.44	15.20	18.44	18.28
$ClHBCl_2H_2Cl$	**51**	24.29	17.68	20.87	15.83	19.02	18.52
H_2BF+HF+H_2O		12.94	11.38	11.33	11.45	11.40	11.42

Table 1 (cont.) *Relative energies (kcal/mol), corrected for zero point vibrational energy differences*

Species		MP2(fu)/ 6-31+G**	MP2/ 6-311+G**	QCISD(T)/ 6-311+G**	MP2/ 6-311+G(3df.2p)	"QCISD(T)"/ 6-311+G(3df.2p)	B3LYP/ 6-311+G**
H_2BF-FH-OH_2	**52**	0.00	0.00	0.00	0.00	0.00	0.00
$H_2BF_2^-$ H_3O^+	**53**	4.26	6.46	6.90	5.13	5.57	5.33
$H_2BF_2^-$+H3O$^+$		150.75	152.68	153.05	152.50	152.87	151.82
H_2BF+HF+NH_3		22.96	17.81	17.57	19.51	19.27	19.18
$H_2BF_2NH_4$	**54**	0.00	0.00	0.00	0.00	0.00	0.00
$H_2BF_2NH_4$	**55**	-0.13	0.01	0.10	0.11	0.21	-0.04
$H_2BF_2NH_4$. bif.	**56**	1.03	0.69	0.80	1.13	1.24	1.22
$H_2BF_2^-$+NH_4^+		119.87	119.48	119.64	121.19	121.35	120.04
H_2BF+HF+CH_3OH		15.71	13.25	12.99	13.70	13.43	13.18
H_2BF-HF-$HOCH_3$	**57**	0.00	0.00	0.00	0.00	0.00	0.00
$H_2BF_2^-$$H_2OCH_3^+$	**58**	1.09	2.44	2.47	1.63	1.65	2.43
$H_2BF_2^-$+$CH_3OH_2^+$		138.08	139.00	138.96	139.26	139.22	137.70
HBF_2+HF+H_2O		13.22	11.68	11.79	11.52	11.63	11.40
HBF_2-FH-OH_2	**59**	0.00	0.00	0.00	0.00	0.00	0.00
HBF_2-FH-OH_2	**60**	0.30	0.11	0.06	0.06	0.00	0.31
$HFBF_2^-$$H_3O^+$	**61**	4.97	8.01	8.11	6.63	6.73	6.88
HBF_3^- H_3O^+	**62**	6.43	9.92	9.73	7.65	7.46	8.70
HBF_3^-+OH_3^+		144.66	147.88	148.28	148.11	148.51	146.87
HBF_2+HF+NH_3		26.67	20.34	20.49	21.91	22.06	20.73
HBF_3^- NH_4^+	**63**	0.00	0.00	0.00	0.00	0.00	0.00
HBF_3^- NH_4^+	**64**	-0.21	0.00	-0.01	-0.21	-0.22	-0.16
HBF_3^-+NH_4^+		117.21	116.90	117.32	119.11	119.54	116.66
HBF_2+HF+CH_3OH		15.84	11.48	11.56	12.22	12.31	12.98
HBF_3^- $H_2OCH_3^+$	**65**	0.00	0.00	0.00	0.00	0.00	0.00
HBF_3^- $H_2OCH_3^+$	**66**	0.55	0.85	0.74	0.60	0.49	2.85
HBF_3^-+$H_2OCH_3^+$		131.84	132.11	132.30	133.32	133.51	132.57
BF_3+HF+H_2O		14.96	13.01	13.24	12.73	12.96	12.57
BF_3-FH-OH_2	**67**	0.00	0.00	0.00	0.00	0.00	0.00
$F_2BF_2^-$ H_3O^+	**68**	4.50	7.53	7.46	6.02	5.95	5.43
FBF_3^- H_3O^+	**69**	5.32	8.77	8.42	6.43	6.08	7.77
BF_4^-+H_3O^+		134.80	138.43	138.71	139.17	139.45	137.49
BF_3+HF+NH_3		31.51	24.64	25.07	26.09	26.51	24.69
FBF_3^- NH_4^+	**70**	0.00	0.00	0.00	0.00	0.00	0.00
FBF_3^- NH_4^+	**71**	-0.20	-0.01	-0.03	-0.20	-0.21	-0.14
BF_4^-+NH_4^+		110.46	110.43	110.89	113.14	113.60	110.07
BF_3+HF+CH_3OH		19.15	14.21	14.62	15.02	15.43	14.47
$F_2BF_2^-$ $H_2OCH_3^+$	**72**	0.00	0.00	0.00	0.00	0.00	0.00
$F_2BF_2^-$ $H_2OCH_3^+$	**73**	0.34	0.56	0.45	0.31	0.21	1.45
BF_4^-+$H_2OCH_3^+$		123.55	124.08	124.35	125.96	126.23	123.50
H_2BCl+HCl+H_2O		2.57	6.00	3.42	8.42	5.84	2.39
$H_2BCl_2^-$ H_3O^+ endo	**74a**	0.00	0.00	0.00	0.00	0.00	0.00
$H_2BCl_2^-$ H_3O^+ exo	**74b**	0.35	0.47	0.46	0.65	0.63	-0.30
$H_2BCl_2^-$ H_3O^+ TS	**75**	0.69	0.89	0.81	0.81	0.73	0.14
$H_2BCl_2^-$+H_3O^+		132.32	135.21	135.01	136.54	136.35	133.61
H_2BCl+HCl+NH_3		20.07	20.99	18.43	23.84	21.27	17.67
$H_2BCl_2^-$ NH_4^+	**76**	0.00	0.00	0.00	0.00	0.00	0.00
$H_2BCl_2^-$ NH_4^+	**77**	1.09	1.57	1.49	1.30	1.22	0.36
$H_2BCl_2^-$+NH_4^+		108.92	110.57	110.37	112.57	112.38	109.36
$HBCl_2$+HCl+H_2O		0.97	4.09	1.32	7.46	4.68	-0.89
$HClBCl_2^-$ H_3O^+	**78a**	0.00	0.00	0.00	0.00	0.00	0.00
$HClBCl_2^-$ H_3O^+	**78b**	2.61	2.51	2.58	3.19	3.26	2.00
$HBCl_3^-$ H_3O^+	**79**	0.07	0.46	0.35	-1.09	-1.19	0.01
$HBCl_3^-$+H_3O^+		126.37	129.26	129.23	131.30	131.28	127.14

Table 1 (cont.) *Relative energies (kcal/mol), corrected for zero point vibrational energy differences*

Species		MP2(fu)/ 6-31+G**	MP2/ 6-311+G**	QCISD(T)/ 6-311+G**	MP2/ 6-311+G(3df.2p)	"QCISD(T)"/ 6-311+G(3df.2p)	B3LYP/ 6-311+G**
$HBCl_2$+HCl+NH_3		21.31	21.74	18.86	25.43	22.54	16.89
$HClBCl_2^-$ NH_4^+	**80**	0.00	0.00	0.00	0.00	0.00	0.00
$HBCl_3^-$ NH_4^+	**81**	-0.37	0.19	0.15	-0.78	-0.81	-0.17
$HBCl_3^-$+NH_4^+		105.80	107.27	107.12	109.88	109.73	105.38
BCl_3+HCl+H_2O		-2.27	0.73	-2.19	4.07	1.14	-5.87
$ClBCl_3^-$ H_3O^+	**82**	0.00	0.00	0.00	0.00	0.00	0.00
$ClBCl_3^-$ H_3O^+	**83**	0.42	0.87	0.74	-0.82	-0.94	0.00
BCl_4^-+H_3O^+		119.53	122.56	122.57	124.54	124.55	119.81

lone pairs. The planar six-membered ring structures have eclipsed conformations as well as wider B-X-H angles than their folded counterparts. Nevertheless, the ring planarization energies are small: only 0.2 kcal/mol for **54** and 1.2 kcal/mol for **76**, see Table 1). Hence, the structures are flexible.

Hardly any folding occurs at the H–H axis in the H_2BX_2 systems: this would (unfavorably) further reduce the X-H-Z (Z=X,O,N) angle (which should be nearly linear for an ideal H-bond). In HBX_3^- and BX_4^- systems, folding at the H-H axis strengthens the additional halogen-hydrogen interaction; this outweighs the weakening of the two other H-bonds.

However, in the H_2BX_2 systems, an interaction between the third nitrogen- or oxygen-bound hydrogen and boron-bound hydrogen is conceivable. Such H–H bonding was recently reported for $(H_2B\text{-}H\cdots H\text{-}NH_2)_2$.[25] Comparison of the two minima computed for H_2BCl_2 H_3O, with the third, oxygen-bound hydrogen toward (**74a**) or away from (**74b**) the boron-bound hydrogen, shows that the energetic contribution is very small at best. **74a** is computed to be 0.6 kcal/mol more stable than **74b**. Transition structrure **75** between **74a** and **74b**, which has an almost planar 6-membered ring, is only 0.1 kcal/mol higher in energy than **74b**.

Conclusion

We showed earlier that acid-base combinations like $NH_3(HX)_n$, X=F, Cl; n=1,2 and, for instance, $NH_3(HCO_2H)$, do not form ion pair (i.e., ionic) structures in the gas phase.[3] The present paper employs high-level *ab initio* computations to identify a number of gas phase ion pairs resulting from interactions of NH_3, H_2O, and CH_3OH with haloboric acids, e.g., HBX_4, X=F, Cl. Although $H^+BX_4^-$ species are not stable entities in the gas phase, the NH_3-HX-BX_3 supermolecules rearrange to $NH_4^+BX_4^-$ and H_2O-HCl-BCl_3 to $H_3O^+BCl_4^-$. These are examples for "salt-like" structures in the gas phase. Bidentate and tridentate ion pair structures have essentially the same energy.

The ability to form ion pairs depends on the intrinsic acidity and basicity of the components, i.e., the proton affinities of the bases and the deprotonation energies of the acids. The relationship between the proton transfer and the deprotonation energies provides a method to predict possible ion pair formation in the gas phase for any acid-base combination. For example, the onset of H_2O protonation was estimated by using $HBCl_3H$ and $HBCl_2H_2$ as models having lower acidity than $HBCl_4$. A water molecule will be protonated in the gas phase by acids or in the solid state by acidic forms of zeolites provided the deprotonation energies ($\Delta H_{DP}[0]$) are lower than 295 kcal/mol.

The structures of the F^- and Cl^- containing bidentate cyclic ion pairs differ distinctly. The six-membered rings with BH_2, BHCl, or BCl_2 groups are strongly bent. The distortion is greater when H···H or H···X hydrogen bonding takes place above the bent ring.

Acknowledgements This work was supported by the Fonds der Chemischen Industrie.

Supplementary Material available Table of total energies (in a.u.) and zero point vibrational energies (ZPE, kcal/mol) in PDF format.

References

1. (a) Bell, R.P. *"The Proton in Chemistry"*, Chapman and Hall, London, 1973. (b) Morrison, R.T.; Boyd, R.N. *"Lehrbuch der Organischen Chemie"*, Verlag Chemie, Weinheim, 1986. (c) Cotton, F.A.; Wilkinson, G. *"Anorganische Chemie"*, Verlag Chemie, Weinheim, 1985. (d) Olah, G.A.; Kuhn, J.S. *J. Am. Chem. Soc.* **1958**, *80*, 6535.
2. Legon, A.C.; Wallwork, A.L.; Rego, C.A. *J. Chem.Phys.* **1990**, *92*, 6397.
3. Heidrich, D.; van Eikema Hommes, N.J.R.; von Ragué Schleyer, P. *J.Comput.Chem.* **1993**, *14*, 1149 and references cited therein.
4. (a) Scrocco, E.; Tomasi, J. *Theor. Chim. Acta* **1975**, *40*, 343. (b) Alagona, G.; Scrocco, E.; Silla, E.; Tomasi, J. *Theor. Chim. Acta* **1977**, *45*, 127. (c) Heidrich, D. *Phys. Chem. Chem. Phys.* **1999**, *1*, 2209.

5. Burkhardt, A.; Wedig, U.; Scholz, G.; Menz, D. *Chem. Phys. Lett.* **1991**, *182*, 556.
6. Krossner, M.; Scholz, G.; Stößer, R. *J. Phys. Chem. A* **1997**, *101*, 1555.
7. (a) Lunsford, J.H.; Rothwell, W.P.; Shen, W. *J. Am. Chem. Soc.* **1985**, *107*, 1540. (b) Earl, W.L.; Fritz, P.O.; Gibson, A.A.V.; Lunsford, J.H. *J. Phys. Chem.* **1987**, *91*, 2091.
8. (a) Teunissen, E.H.; van Santen, R.A.; Jansen, A.P.J.; van Duijneveldt, F.B. *J. Phys. Chem.* **1993**, *97*, 203. (b) Kassab, E.; Fouquet, J.; Allavena, M.; Evleth, E.M. *J. Chem. Phys.* **1993**, *97*, 9034.
9. van Santen, R.A.; Kramer, G.J. *Chem. Rev.* **1995**, *95*, 637 and references cited therein.
10. Batamack, P.; Doremieux-Morin, C.; Fraissard, J. *J. Chem. Phys.* **1992**, *89*, 423. (b) Batamack, P.; Doremieux-Morin, C.; Fraissard, J.; Freude, D. *J. Phys. Chem.* **1991**, *95*, 3790. (c) Batamack, P.; Doremieux-Morin, C.; Vincent, R.; Fraissard, J. *Chem. Phys. Lett.* **1991**, *180*, 545. (d) Kubelkova, L.; Novakova, J.; Nedomova, K. *J. Catal.* **1990**, *124*, 441.
11. (a) Gale, J.D.; Catlow, C.R.A.; Carruthers, J.R. *Chem. Phys. Lett.* **1993**, *216*, 155. (b) Haase, F.; Sauer, J. *J. Phys. Chem.* **1994**, *98*, 3083 (c) Haase, F.; Sauer, J. *J. Am. Chem. Soc.* **1995**, *117*, 3780. (d) Blaszkowski, S.R.; van Santen, R.A. *J. Phys. Chem.* **1995**, *99*, 11728 and references therein, (e) Nusterer, E.; Blöchl, P.E.; Schwarz, K. *Chem. Phys. Lett* **1996**, *253*, 448.
12. (a) Pelmenschikov, A.G.; van Santen, R.A.; *J. Chem. Phys.* **1993**, *97*, 10678. (b) Smith, L.; Cheetham, A.K.; Morris, R.E.; Marchese, L.; Thomas, J.M.; Wright, P.A.; Chen, J. *Science* **1996**, *271*, 799. (c) Wakabayashi, F.; Kondo, J.N.; Domen, K.; Hirose, Ch. *J. Phys. Chem.* **1996**, *100*, 1442.
13. Sauer, J. *Science* **1996**, *271*, 774.
14. Suresh, C.H.; Gadre, S.R.; Gejji, S.P. *Theor. Chem. Acc.* **1998**, *99*, 151.
15. Gaussian 98, Revision A.5: Frisch, M. J.; Trucks, G. W.; Schlegel, H. B.; Scuseria, G. E.; Robb, M. A.; Cheeseman, J. R.; Zakrzewski, V. G.; Montgomery, J. A. , Jr.; Stratmann, R. E.; Burant, J. C.; Dapprich, S.; Millam, J. M.; Daniels, A. D.; Kudin, K. N.; Strain, M. C.; Farkas, O.; Tomasi, J.; Barone, V.; Cossi, M.; Cammi, R.; Mennucci, B.; Pomelli, C.; Adamo, C.; Clifford, S.; Ochterski, J.; Petersson, G. A.; Ayala, P. Y.; Cui, Q.; Morokuma, K.; Malick, D. K.; Rabuck, A. D.; Raghavachari, K.; Foresman, J. B.; Cioslowski, J.; Ortiz, J. V.; Stefanov, B. B.; Liu, G.; Liashenko, A.; Piskorz, P.; Komaromi, I.; Gomperts, R.; Martin, R. L.; Fox, D. J.; Keith, T.; Al-Laham, M. A.; Peng, C. Y.; Nanayakkara, A.; Gonzalez, C.; Challacombe, M.; Gill, P. M. W.; Johnson, B.; Chen, W.; Wong, M. W.; Andres, J. L.; Gonzalez, C.; Head-Gordon, M.; Replogle, E. S.; Pople, J. A., Gaussian, Inc., Pittsburgh PA, **1998**.
16. (a) Curtiss, L.A.; Raghavachari, K.; Trucks, G.W.; Pople, J. A. *J. Chem. Phys.* **1991**, *94*, 7221. (b) Curtiss, L.A.; Raghavachari, K.; Pople, J.A. *J. Chem. Phys.* **1992**, *98*, 1293.
17. Reed, A.E.; Weinhold, F.; Curtiss, L.A. *Chem. Rev.* **1988**, *88*, 899.
18. Sauer, J.; Ugliengo, P.; Garrone, E.; Saunders, V.R. *Chem. Rev.*, **1994**, *94*, 2095.
19. Phillips, J.A.; Canagaratna, M.; Goodfriend, H.; Grushow, A.; Almlöf, J.; Leopold, K.R. *J. Am. Chem. Soc.* **1995**, *117*, 12549 and literature therein.
20. (a) Takeo, H.; Sugie M.; Matsumura, C. *J. Mol. Spectrosc.* **1993**, *158*, 201. (b) Kawashima, Y.; Takeo, H.; Sugie, M.; Matsumura, C.; Hirota, E. *J. Chem. Phys.* **1993**, *99*, 820.
21. Oswald, M.; Flügge, J.; Botschwina, P. *J. Mol. Structure* **1994**, ***320***, 227 and literature therein.
22. van Eikema Hommes, N.J.R. unpublished.
23. (a) Ceyer, S.T.; Tiedemann, P.W.; Mahan, B.H.; Lee, Y.T. *J. Chem. Phys.* **1979**, *70*, 14. (b) East, A.L.L.; Smith, B.J.; Radom, L. *J. Am. Chem. Soc.* **1997**, *119*, 9014 and literature therein.
24. c.f. (a) von Ragué Schleyer, P.; West, R. *J. Am. Chem. Soc.* **1959**, *81*, 3164. (b) West, R.; Powell, D.L.; Whatley, L.S.; Lee, M.K.T. *J. Am. Chem. Soc.* **1962**, *84*, 3221.
25. Richardson, T.B.; de Gala, S.; Crabtree, R.H. *J. Am. Chem. Soc.* **1995**, *117*, 12875.

Appendix: Overview of structures

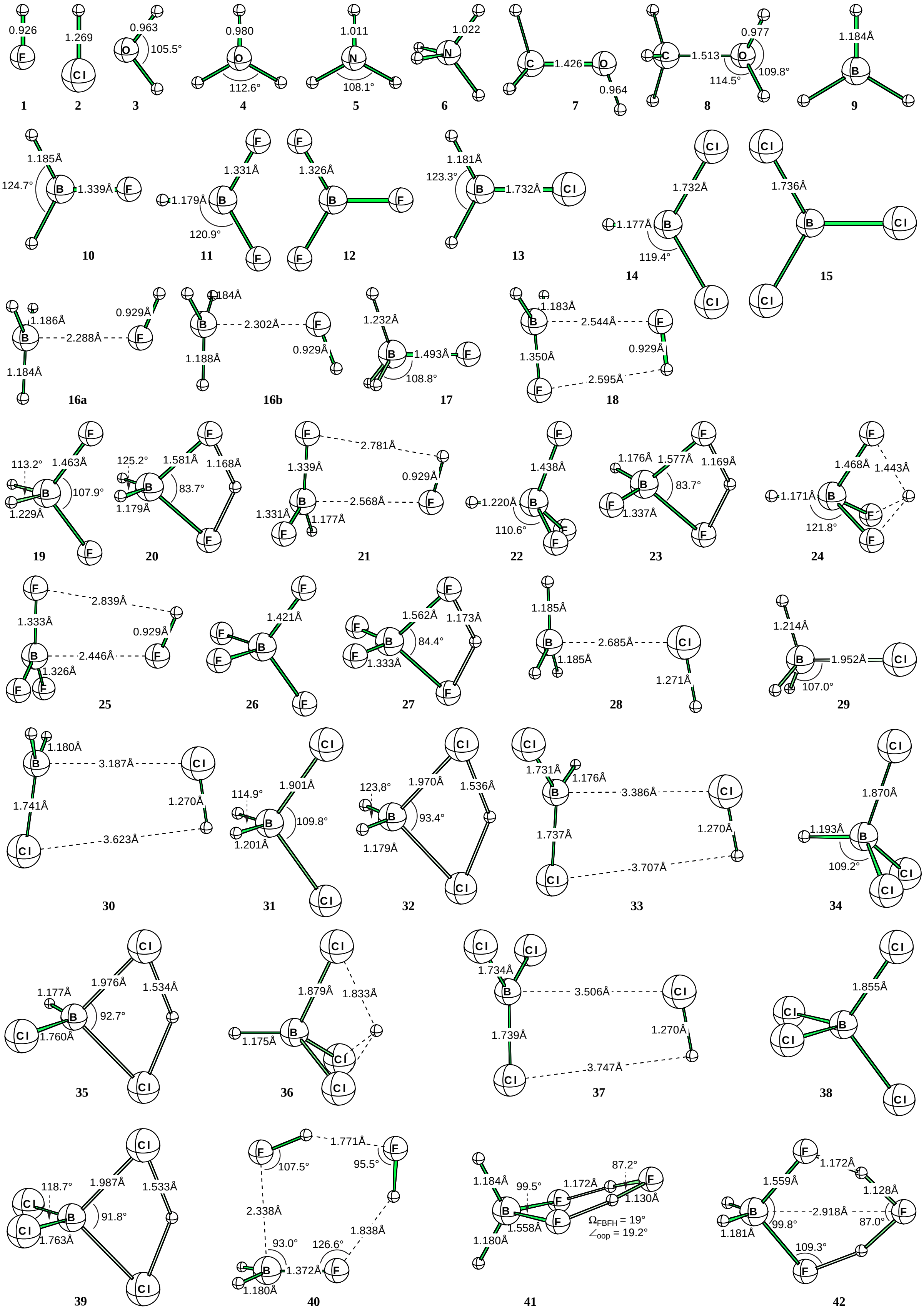

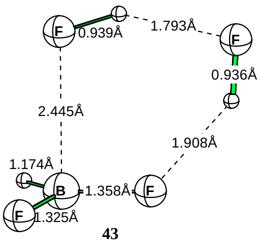

43

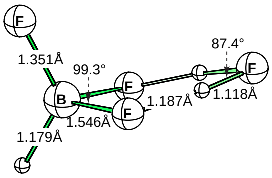

44

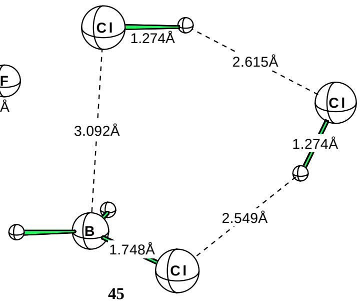

45

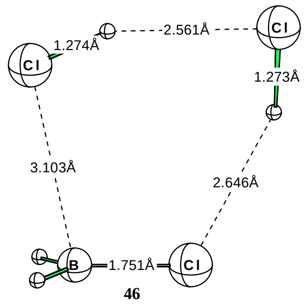

46

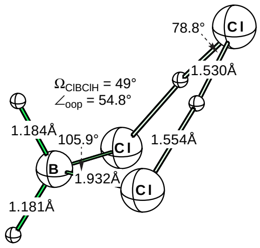

47

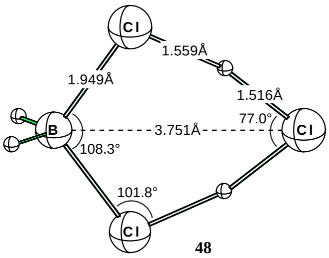

48

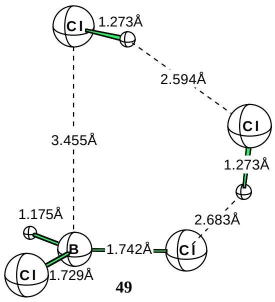

49

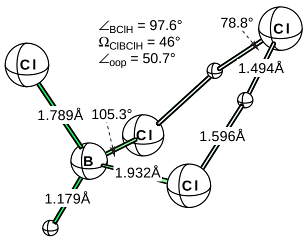

50

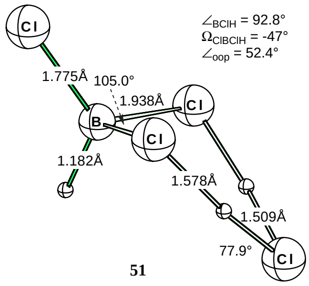

51

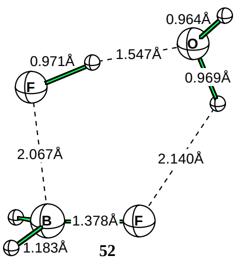

52

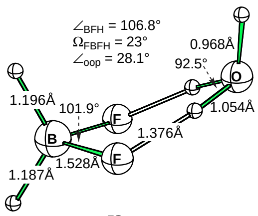

53

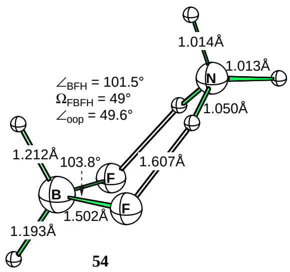

54

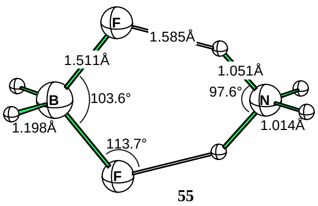

55

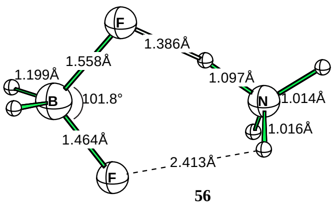

56

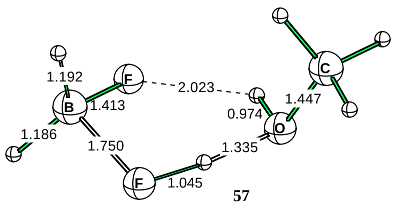

57

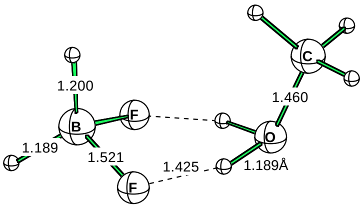

58

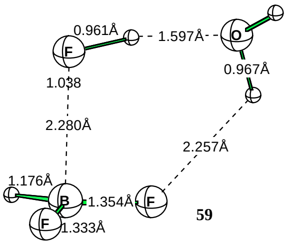

59

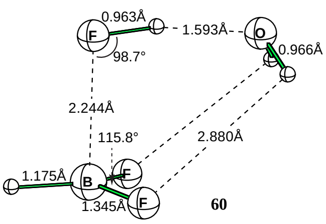

60

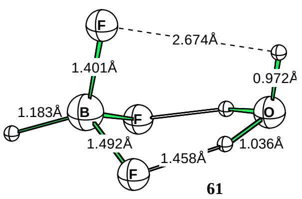

61

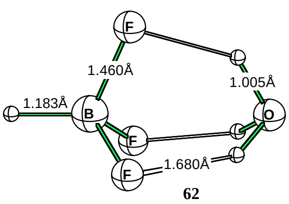

62

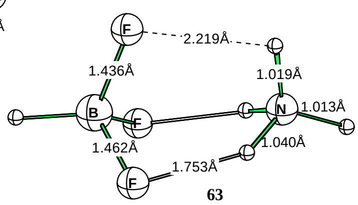

63

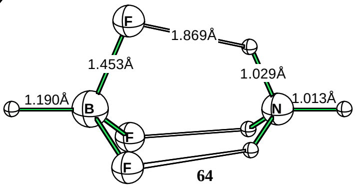

64

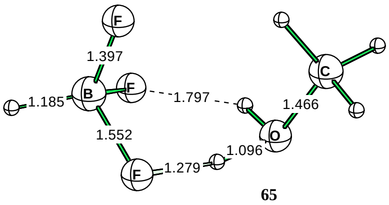

65

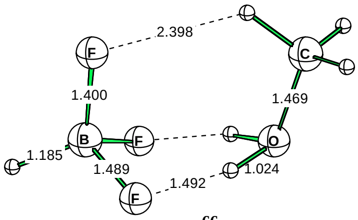

66

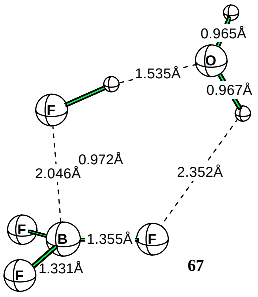

67

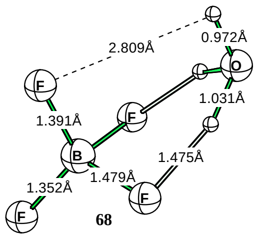

68

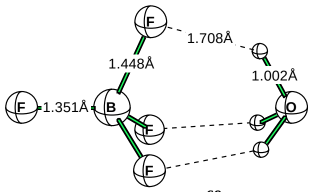

69

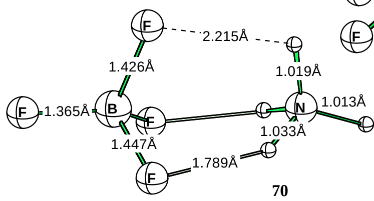

70

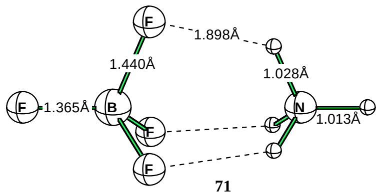

71

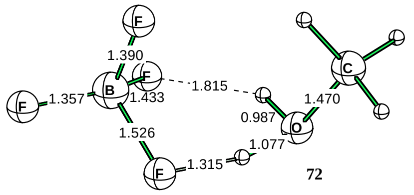

72

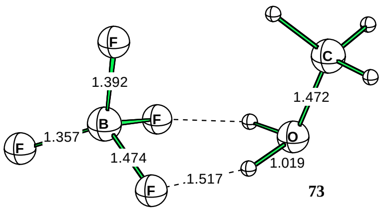

73

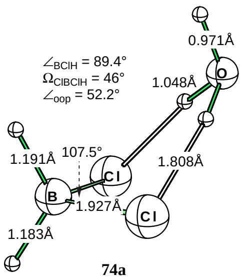

74a

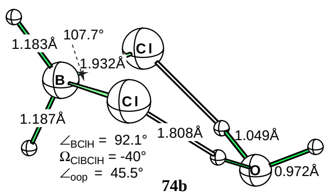

74b

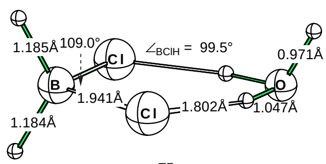

75

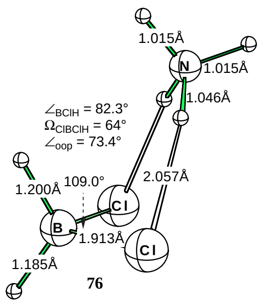

76

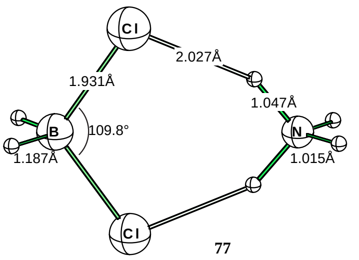

77

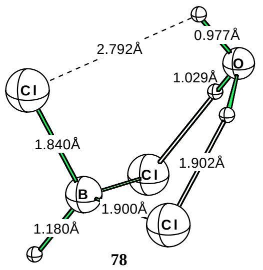

78

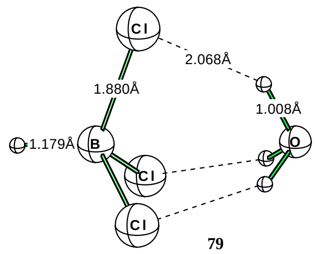

79

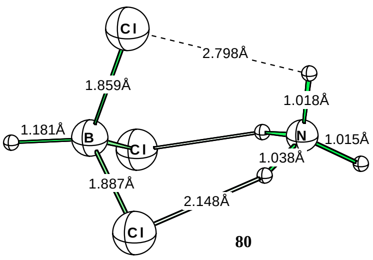

80

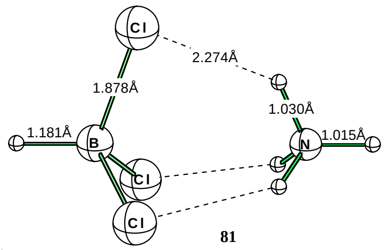

81

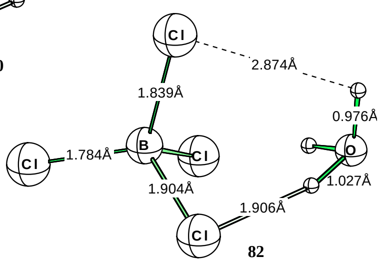

82

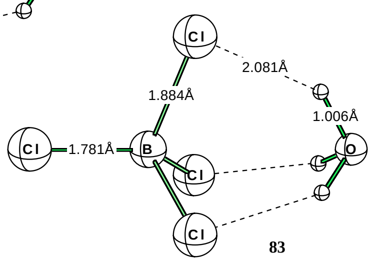

83